Realizability improvements to a hybrid mixture-bubble model for simulation of cavitating flows

Citation for the original published paper (version of record):
Ghahramani, E., Arabnejad Khanouki, M., Bensow, R. (2018)
Realizability improvements to a hybrid mixture-bubble model for simulation of cavitating flows
Computers and Fluids, 174: 135-143
http://dx.doi.org/10.1016/j.compfluid.2018.06.025

Computers and Fluids 174 (2018) 135–143

Contents lists available at ScienceDirect

Computers and Fluids

journal homepage: www.elsevier.com/locate/compfluid

Realizability improvements to a hybrid mixture-bubble model for simulation of cavitating flows

Ebrahim Ghahramani*, Mohammad Hossein Arabnejad, Rickard E. Bensow

Department of Mechanics and Maritime Sciences, Chalmers University of Technology, Gothenburg 412 96, Sweden

ARTICLE INFO

Article history:
Received 20 February 2018
Revised 21 June 2018
Accepted 25 June 2018
Available online 7 July 2018

Keywords:
Cavitating flow
Disperse multiphase flow
Multi-scale model

ABSTRACT

Cavitating multi-phase flows include an extensive range of cavity structures with different length scales, from micro bubbles to large sheet cavities that may fully cover the surface of a device. To avoid high computational expenses, incompressible transport equation models are considered a practical option for simulation of large scale cavitating flows, normally with limited representation of the small scale vapour structures. To improve the resolution of all scales of cavity structures in these models at a moderate additional computational cost, a possible approach is to develop a hybrid Eulerian mixture -Lagrangian bubble solver in which the larger cavities are considered in the Eulerian framework and the small (sub-grid) structures are tracked as Lagrangian bubbles. A critical step in developing such hybrid models is the correct transition of the cavity structures from the Eulerian mixture to a Lagrangian discrete bubble framework. In this paper, such a multi-scale model for numerical simulation of cavitating flows is described and some encountered numerical issues for Eulerian–Lagrangian transition are presented. To address these issues, a new improved formulation is developed, and simulation results are presented that show the issues are overcome in the new model.

1. Introduction

Cavitation is a common phenomenon in industrial hydraulic systems, such as marine propulsion systems and fuel injectors. It is in many cases an undesirable and unavoidable occurrence. One issue is material loss and degradation due to cavitation erosion, which is believed to be the result of violent and very fast collapses of the generated vapour micro-bubbles. Moreover, cavitation is often accompanied by issues of noise, vibrations, load variations and loss of efficiency in hydraulic devices such as propellers and pumps. Multiphase cavitating flows contain an extensive range of cavity structures with different length scales. A sheet cavity that fully or partially cover the suction side of a hydrofoil may break up into smaller cloud cavities and micro bubbles which are further transported into regions of higher pressure, where collapse-like condensation results in the formation of liquid jets and pressure shocks. Due to the mentioned significance and complexity of the flow field, understanding and controlling cavitation has been a major challenge in engineering in recent decades.

Computational Fluid Dynamics (CFD) simulation, as a supplement or alternative to experimental measurements, can give a more comprehensive understanding of the hydrodynamics of cavitation erosion. Various numerical methods are being used by different researchers today and most of them can be categorized into two general approaches. The first approach is based on the mixture equation of state, assuming thermodynamic equilibrium (e.g. [1,2]). This approach requires very small time steps since it considers compressible liquid and vapour phases and it limits the applications of the model [3]. Therefore, even if there are suitable models that can adequately estimate the behaviour of vapour structures, their application in industrial problems (e.g. marine propellers) is limited, as they require substantial computational resources and long simulation times.

The second approach is based on a transport equation for vapour or liquid fraction, incorporating models for vapourization and condensation. Various numerical models are included in this general classification which may be further categorized into different groups, e.g. compressible or incompressible approaches. Also, the transport equation may be developed in both Eulerian and Lagrangian viewpoints to track the vapour structures and their interactions with the liquid phase. In the Eulerian models (e.g. [4–8]), the multiphase flow is usually treated as a single

* Corresponding author.
E-mail address: ebrahim.ghahramani@chalmers.se (E. Ghahramani).

https://doi.org/10.1016/j.compfluid.2018.06.025

fluid mixture and mass transfer between the phases is defined by explicit source terms. This method performs rather well in regions with moderate flow changes but in zones of strong, vortical flow, they cannot capture cavity transport accurately. A major reason is that, typically, these models utilise an asymptotic form of the well-known Rayleigh–Plesset equation of bubble dynamics [9]. Another limitation of this model (as well as other Eulerian approaches) is that vapour structures smaller than the grid size, such as cavitation nuclei and bubbles, or sparse clouds of bubbles, cannot be handled very well.

The Lagrangian models (e.g. [10]), on the other hand, enable more detailed formulations for transport, dynamics, and acoustics of discrete vapour bubbles. As this group of models are developed based on a more accurate form of the Rayleigh–Plesset equation, they can have a more precise estimation of the dynamics of cavitating flows with large values of vorticity and pressure gradients. While the bubble sizes in this viewpoint can be much smaller than the grid size, these models are computationally expensive when the number of bubbles is large. Further, this approach is limited in representation of large or non-spherical vapour structures.

Considering the above mentioned capabilities and limitations of the Eulerian and Lagrangian formulations, a solution can be to develop a hybrid model that is capable in both resolving the large vapour structures through a mixture approach, and capturing the small-scale structures as discrete bubbles (e.g. [11]). In this paper, such a hybrid mixture-bubble model is implemented in OpenFOAM. In this model, the large vapour structures are handled using the Eulerian single fluid mixture method and the small scale spherical bubbles are tracked in the Lagrangian framework. This model is similar to the work of Vallier [12], in turn inspired by the study of Tomar et al. [13]. However, new development presented in this study includes improvements in some features including the continuity and volume fraction equations as well as the calculation of mixture properties. This is a multi-scale model to simulate cavitating flows with different length scales.

In general, in multi-phase flows, using multi-scale simulation models is a popular approach and numerous studies can be found in literature. For example, Tomiyama and Shimada [14] proposed a (N+2)-field modeling approach which can deal with two continuous phase fields and N dispersed gas phase fields. Also, Černe et al. [15] and Štrubelj and Tiselj [16] developed another model by coupling of an interface capturing Volume of Fluid (VOF) based method with the two-fluid model, so that in parts of the domain where the flow was too dispersed to be described by the interface capturing algorithms, the two-fluid model was used. However, as explained before, Eulerian approaches are limited in capturing small bubble dynamics with reasonable computational expense and most of the developed multi-scale models in literature are Eulerian–Eulerian solvers. The concept of multi-scale hybrid Eulerian–Lagrangian solvers is a more recent approach to simulate multiphase flows in large scale applications for which effective small scale details need to be represented sufficiently well. This methodology has gained more popularity in recent years for simulation of atomizing gas-liquid flows [17]. The works of Kim et al. [18], Herrmann [19] and Tomar et al. [13] are the pioneering efforts to couple the Lagrangian Particle Tracking (LPT) with interface capturing schemes, such as Level Set [19] and VOF [13]. Also, Ling et al. [20] developed a hybrid model with more emphasis on the correction of momentum equation source terms due to the Eulerian–Lagrangian coupling in order to accurately compute the dynamics of the Lagrangian droplets that are larger than the grid spacing. In that study, the Eulerian structures are directly converted to one Lagrangian droplet with equal volume (similar to Tomar et al. [13]), but only a special zone of the flow domain is subjected to this conversion and thin ligaments and sheets are exempted from this treatment. In addition to the direct transition from Eulerian to Lagrangian structures, there are statistical algorithms (e.g. [21]) in which the transfer of mass from Eulerian to Lagrangian framework is done via a statistical model, tuned to the upstream predictions of the Eulerian model. This method reduces the computational time in comparison to the previous method, but some of the information (positions, mass, momentum) may not be preserved during the transition. Also, Ström et al. [22] used a switching zone with a statistical method which is designed to ensure that the Lagrangian parcels exit the zone with the correct statistics. The advantage of this approach was that the computationally demanding resolution of the liquid primary atomization process could be avoided altogether.

The mentioned Eulerian–Lagrangian hybrid models have been developed for atomizing gas-liquid flows. However, this approach can be utilized for cavitating flows as well. For example, Hsiao et al. [23] and Ma et al. [24] have developed a model with coupling of a Lagrangian Discrete Singularities Model and an Eulerian level set approach. In these studies, the Eulerian cavities are directly transformed to Lagrangian bubbles, but the bubble volume is spread smoothly over neighbouring cells within a selected radial distance. There are important distinctions between cavitating flow and atomizing flow applications which should be considered in model developments. In the mentioned hybrid models for atomizing flows (except [22]), it has been assumed that the Lagrangian particles do not occupy any volume in the Eulerian description which is valid when the Lagrangian formulation is used only in the dilute regions of a flow. Also, the resulting model will be useful in situations where continuous phase density is very low in comparison to the dispersed phase density [22], such as liquid spray applications. However, in cavitating flows we encounter the opposite case since the continuous phase density (water) is much larger than the (vapour) bubble density and such an assumption is not valid. Besides that, in liquid atomizers, the dilute dispersed flow and the continuous two-phase flows are present in separate regions of the domain as the dispersed droplets are the result of the break-up of the two-phase structures in the downstream; this makes the numerical implementation of the transition algorithm more convenient. In contrast, in cavitating flows, at each point of the two-phase regime both small bubbles as well as large Eulerian cavities can be present. Another significant difference between the two applications is that in atomized liquids, for direct transition, each liquid fragment is usually converted into one Lagrangian droplet with equal volume, while in cavitating flows, each Eulerian structure is actually a cloud of bubbles or a bubbly mixture and its properties (e.g. density) are not equal to the pure vapour (dispersed phase) properties. Therefore, the cavity might be replaced by a group of smaller bubbles (instead of one larger bubble) in such a way that the properties of the combined bubble group are equal to the corresponding values of the old Eulerian cavity. Vapour condensation / liquid vapourization is a mass transfer process which only happens in cavitating flows, adding the need for modelling mass transfer in the governing equations. As stated before, a key factor in developing such solvers is the correct and smooth transition between Lagrangian and Eulerian structures and it is more important in cavitating flow simulations. When an Eulerian mixture structure is transformed to a Lagrangian bubble or vice versa, since the related transport equation to track the structure is modified, a wrong transition process may cause drastic non-continuous changes and spurious pressure pulses in the domain.

In the current paper, the coupling of the Lagrangian library with a mixture-based Eulerian solver is described in some detail, with focus on the correct definition of the transition process and the improved Eulerian governing equations. In this solver the condensation / vapourization source terms are considered in the governing equations and there is no need to distribute bubble volume over the neighbouring cells. The new model is developed in

the open source C++ package OpenFOAM by improving the interPhaseChangeFOAM solver and coupling it with a Lagrangian library, developed based on the available Lagrangian models in OpenFOAM [25].

In the following sections, the general Eulerian mixture model, the Lagrangian bubble model, and their coupling are described first. Then the main issue in the transition process is explained and the proposed formulation to overcome this issue is developed. Finally a qualitative and quantitative validation of the improved model performance is presented.

2. Method

2.1. Eulerian mixture model

In this model, the vapour and liquid phases are treated as a single mixture fluid fully in an Eulerian framework, where the continuity equation and one set of momentum equations for the mixture are solved. We here consider an incompressible flow model, motivated by the balance of computational cost and model accuracy for the intended applications as described above, but a similar framework can be developed for compressible flows.

The continuity equation is then given by

$$\frac{\partial u_i}{\partial x_i} = \left(\frac{1}{\rho_l} - \frac{1}{\rho_v}\right)\dot{m}. \tag{1}$$

The RHS term is the effect of vapourization and condensation, where $\dot{m}$ is the rate of mass transfer between phases, ρ_l is the liquid density and ρ_v is the vapour density. Further, the Navier–Stokes equations are

$$\frac{\partial(\rho_m u_i)}{\partial t} + \frac{\partial\left(\rho_m u_i u_j\right)}{\partial x_j} = \frac{\partial \tau_{ij}}{\partial x_j} + \rho_m g_i. \tag{2}$$

Here, ρ_m and τ_{ij} are the mixture density and the stress tensor, respectively, which are defined as

$$\rho_m = \alpha\rho_l + (1-\alpha)\rho_v, \tag{3}$$

$$\tau_{ij} = -p\delta_{ij} + \mu_m\left(\frac{\partial u_i}{\partial x_j} + \frac{\partial u_j}{\partial x_i} - \frac{2}{3}\frac{\partial u_k}{\partial x_k}\delta_{ij}\right), \tag{4}$$

where μ_m is the mixture dynamic viscosity, given by

$$\mu_m = \alpha\mu_l + (1-\alpha)\mu_v, \tag{5}$$

and α is the liquid volume fraction which specifies the relative amount of liquid in a given volume, e.g. a computational cell. In the Eulerian approach, the evolution of the volume fraction is calculated by solving a scalar transport equation given as

$$\frac{\partial \alpha}{\partial t} + \frac{\partial(\alpha u_i)}{\partial x_i} = \frac{\dot{m}}{\rho_l}. \tag{6}$$

To close the above set of equations the mass transfer rate, $\dot{m}$, should be determined. There are many numerical models in literature to estimate this term and most of them are based on a simplified form of the well-known Rayleigh–Plesset equation. In this study, the Schnerr–Sauer model [26] is used, but the methodology for the hybrid solver does not rely on this particular choice of mass transfer model. The vapourization and condensation rates are then given by

$$\begin{aligned}
\dot{m}_c &= C_c\alpha(1-\alpha)\frac{3\rho_l\rho_v}{\rho_m R_B}\sqrt{\frac{2}{3\rho_l|p-p_{threshold}|}}\max(p-p_{threshold},0),\\
\dot{m}_v &= C_v\alpha(1+\alpha_{Nuc}-\alpha)\\
&\quad\times\frac{3\rho_l\rho_v}{\rho_m R_B}\sqrt{\frac{2}{3\rho_l|p-p_{threshold}|}}\min(p-p_{threshold},0),
\end{aligned} \tag{7}$$

where $\dot{m}_c$ and $\dot{m}_v$ are the rates of condensation and vapourization, respectively, and $\dot{m} = \dot{m}_c + \dot{m}_v$. In the above equations, R_B and α_{Nuc} are user defined model parameters corresponding to generic radius and volume fraction of bubble nuclei in the liquid. Also, $p_{threshold}$ is a threshold pressure at which the phase change is assumed to happen, usually considered as the vapour pressure of the fluid.

One feature of this Eulerian approach is that it treats the structures that are smaller than the grid size as a homogeneous mixture, therefore sparse vapour clouds or sub-grid inhomogeneity in cavitation clouds are not well treated. An extremely high mesh resolution is required to resolve small individual cavitation bubbles. Besides that, during the last steps of the cavity collapse and early stages of its rebound, the cavity size changes very rapidly and since the Eulerian approaches are based on a simplified form of the Rayleigh–Plesset equation, they cannot give an accurate estimation of the cavity inertia. Thus, as a solution, a combination of the Eulerian mixture formulation, for the macroscopic development, with a Lagrangian model, to account for evolution of small scale structures, may be developed, aiming for a more realistic estimation of the whole range of cavity sizes.

2.2. Discrete bubble model

In this model, the cavities are treated as discrete (possibly parcels of) Lagrangian bubbles transported in an ambient Eulerian continuous flow. At each time step, the Eulerian equations are solved first and then the bubbles are tracked by solving a set of ordinary differential equations along the bubbles trajectories, given by

$$\begin{aligned}
\frac{dx_{b,i}}{dt} &= u_{b,i},\\
m_b\frac{du_{b,i}}{dt} &= F_d + F_l + F_a + F_p + F_b + F_g.
\end{aligned} \tag{8}$$

The RHS of the second equation includes various forces that are exerted on the bubbles which are, from left to right, sphere drag force [27], Saffman–Mei lift force [28], added mass, pressure gradient force, buoyancy force, and gravity; the latter terms are naturally expressed through the model formulation. These forces typically depend on the bubble size. Explicit inclusion of all relative forces is another advantage of the Lagrangian model which gives the opportunity to consider different flow effects on cavity behaviour.

The variation of bubble size is calculated by solving the Rayleigh–Plesset equation (see [29,30]),

$$R(t)\ddot{R}(t) + \frac{3}{2}\dot{R}^2(t) = \frac{p_B - p}{\rho_m} - 4\nu_m\frac{\dot{R}(t)}{R(t)} - \frac{2\sigma_{st}}{\rho_m R(t)}, \tag{9}$$

where R is the bubble radius, p_B is the bubble inside pressure, p is the fluid pressure, and σ_{st} is the surface tension. In this study, the time-step adaptive second-order Rosenbrock method is implemented to solve the Rayleigh–Plesset equation numerically (see e.g. [31] for a description of this approach). Most of the popular Eulerian explicit mass transfer models, including the Schnerr–Sauer model described above, are derived based on an asymptotic form this equation in which the first term on the left hand side is ignored for simplicity. As stated before, such a simplification may affect the cavity inertia at the last steps of the collapse or early stages of its rebound.

An important issue in the tracking of Lagrangian bubbles that should be considered, is the relative sizes of bubbles and grid cells. Sometimes (e.g. when a new bubble is injected) a bubble may be larger and occupy a number of cells. In OpenFOAM, when a bubble approaches a wall, the wall boundary condition is applied correctly only if the bubble size is smaller than the wall cell height. Therefore, to have a correct prediction of wall boundary condition for

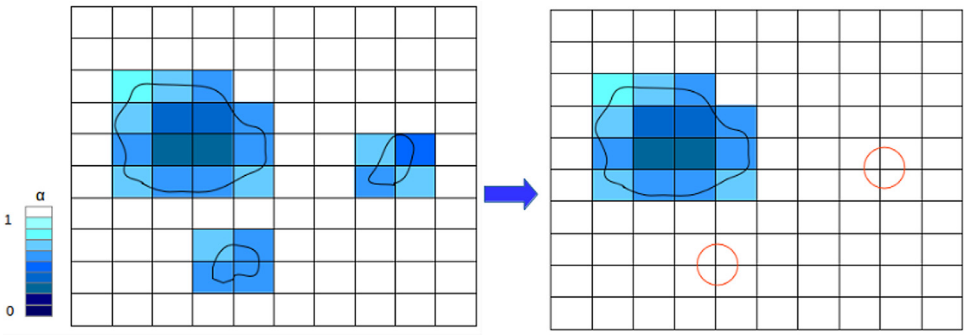

Fig. 1. Transition of small cavities to Lagrangian bubbles. (For interpretation of the references to colour in this figure legend, the reader is referred to the web version of this article.)

bubbles, a second coarser grid, should be used for bubble tracking as the aspect ratio of wall cells increases in a viscous flow simulation. Therefore, at each time step the continuous flow field equations are solved in the main grid and then the obtained Eulerian values are transformed to the coarser grid to track the bubbles. Note that this is a limitation in the current formulation in OpenFOAM, and not necessarily a general issue with a Lagrangian bubble model.

Since the dispersed phase (Lagrangian bubbles) in the cavitating flow is locally dense, and have properties quite different from liquid properties, the bubbles have considerable effect on the ambient flow field, similar to Eulerian cavities. Thus the Eulerian–Lagrangian computations should be based on four-way coupling. In other words, both the bubble-bubble and bubble-flow interactions should be considered. In the current methodology, the bubble-bubble interaction is considered through implementation of bubble-bubble collision; after a collision, a pair of bubbles may coalesce to form a larger bubble or they may bounce back from each other and this is specified based on the bubbles relative velocity and the interaction time. The bubble-flow interaction can be implemented in the Eulerian equations in different ways that in large define the characteristics of the hybrid model. This is further expanded in the following sections.

2.3. The multi-scale hybrid solver

In the multi-scale solver, the cavities are categorized as Eulerian structures and Lagrangian bubbles. At each time step, small Eulerian cavity structures (normally representing a cluster of bubbles) that are not resolved by sufficient number of computational cells, are transformed to Lagrangian bubbles. Thus, the corresponding Eulerian liquid volume fraction of the respective cells (α) needs to be set equal to 1. This transition is shown schematically in Fig. 1 for a simple grid. The grid cells that have Eulerian cavities are coloured blue with $\alpha < 1$. Two of the cavities are resolved only by four cells and they are replaced by Lagrangian bubbles. Also, if a bubble later becomes large enough or it hits an Eulerian cavity, it is transformed back to a Eulerian structure by deleting the bubble and setting a corresponding new α value in the occupied cells.

In the common straight-forward manner, when an Eulerian vapour structure is replaced by a bubble, the liquid volume fraction values (α) in the respective cells is set to 1; see e.g. [12]. This sudden change will cause a jump in the values of the mixture properties, ρ_m and μ_m, based on the Eqs. (3) and (5). Since there is a significant difference between the values of the liquid and vapour properties, this jump is considerable. Besides that, the mass transfer rate, $\dot{m}$, experiences a sudden change after removing an Eulerian vapour structure Eq. (7). Such significant changes in the flow properties and the continuity equation source term can cause spurious numerical pressure pulses which may have significant unrealistic effects on the flow field. For example, these pulses can decrease the local pressure in the cavitating region which leads to generation of new vapour structures. Also, spurious pressure pulses have negative effect on the noise prediction and erosion estimation of the flow.

Therefore the Eulerian governing equations should be modified to both avoid the spurious pressure pulse problem and while still consider the bubble effect on the continuous flow.

2.4. The realizable hybrid mixture-bubble model

To avoid the issue described above, the coupling between the bubbles and the Eulerian mixture flow needs to be reconsidered. There are two methods to implement the bubble effect on the Eulerian flow field. One approach is to consider the bubbles as a separate phase by defining a new void fraction for them and apply the bubble effect through correct implementation of this parameter in the Eulerian equations (Eqs. (1), (2) and (6)). Also, the bubble reacting force should be applied directly as a source term in the Navier–Stokes equation. This approach is used by, e.g., Ström et al. [22]. A simpler approach is to implement the bubble effect by modifying the volume fraction contribution in the calculation of mixture properties and phase change rate (Eqs. (3), (5) and (7)). In this latter approach, the mixture properties and phase change rate are affected not only by the Eulerian vapour cavities, but also by the Lagrangian bubbles volume fraction in the domain. In other words, the mixture approach is the same as before, but now some of the vapour structures are tracked by solving the Eulerian transport equation and some of them are treated as discrete Lagrangian bubbles. Then the vapour volume fraction is obtained from the distribution of both of the Eulerian cavities and Lagrangian bubbles. It is important to note that the Lagrangian bubbles do not constitute a second phase, but they contribute as vapour structures in the mixture fluid; therefore, there is no inter-phase momentum transfer term to be considered in the Navier–Stokes equations. Due to its simplicity, the later approach is used in this study. Hsiao et al. [23] used the same method to calculate new mixture properties.

In order to avoid spurious pressure pulse problems and create a smooth and physically reasonable transition, three improvements have been developed: the joint representation of the phases in the mixture framework; a careful introduction of bubbles in relation to cell size and mixture distribution; and attention to mass transfer in presence of discrete bubbles. Starting with the first item, mixture properties and phase change rate should be defined based on a new term which is similar to α but that does not change during Eulerian–Lagrangian transition. In each bubbly cell, the cell volume is occupied by both fluid and bubbles. The fluid contribution in the cell is defined by a new parameter which is called β; similarly the bubble volume fraction in the cell is $1-\beta$. It is obvious that in cells containing bubbles, β is less 1, while it is equal to

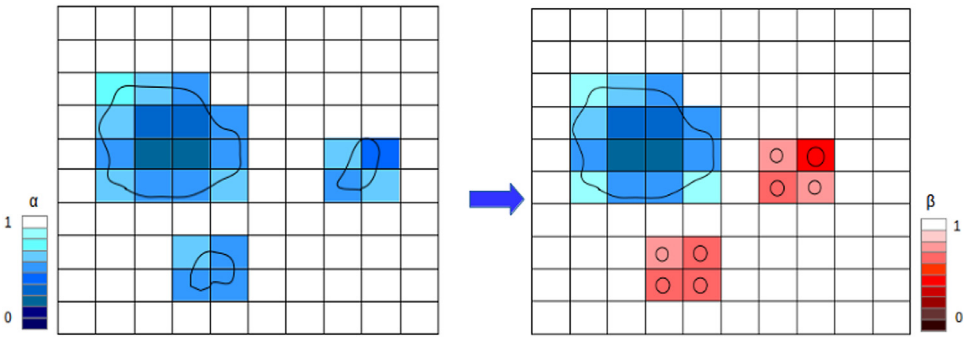

Fig. 2. Improved transition; the numbers show the α value is the left image and the β value in the right image .(For interpretation of the references to colour in this figure legend, the reader is referred to the web version of this article.)

1 everywhere else. During the Eulerian to Lagrangian transition, a vapour structure which occupies $(1-\alpha)$ fraction of the hosting cells is replaced by a bubble which occupies $(1-\beta)$ fraction of the same cells. Therefore the new value of β in the host cells is the same as the old value of α. Also, the new value of α is 1 which is exactly the same as the old value of β since there were no bubbles in the host cells before the transition. In other words, both α and β have similar sudden changes, however their product $\alpha\beta$ does not change during the Eulerian–Lagrangian transition. In the bubble cells, where $\alpha = 1$, $\alpha\beta$ has the same value as β and everywhere else it is equal to α. Consequently, this parameter is suitable to replace α in the definition of mixture properties and calculation of phase change rate, $\dot{m}$. Therefore, the mixture properties formula can be modified as

$$\begin{aligned} \rho_m &= \alpha\beta\rho_l + (1-\alpha\beta)\rho_v, \\ \mu_m &= \alpha\beta\mu_l + (1-\alpha\beta)\mu_v. \end{aligned} \tag{10}$$

Further, the phase change rate formula is modified as

$$\begin{aligned} \dot{m}_c &= C_c\alpha\beta(1-\alpha\beta) \\ &\quad \times \frac{3\rho_l\rho_v}{\rho_m R_B}\sqrt{\frac{2}{3\rho_l|p-p_{threshold}|}}\max(p-p_{threshold},0), \\ \dot{m}_v &= C_v\alpha\beta(1+\alpha_{Nuc}-\alpha\beta) \\ &\quad \times \frac{3\rho_l\rho_v}{\rho_m R_B}\sqrt{\frac{2}{3\rho_l|p-p_{threshold}|}}\min(p-p_{threshold},0). \end{aligned} \tag{11}$$

Using the above equation avoids drastic changes in the mixture flow representation and large spurious pressure pulses in the flow.

Continuing with the second correction needed in the multi-scale solver we note that during transition, in each cell of the host cells group, the new value of β should be exactly equal to the old value of α to keep the $\alpha\beta$ parameter conserved. In other words, the bubble contribution in each cell should be equal to the contribution of the corresponding Eulerian cavity. However, while the summation of cavity contribution (old α) is the same as the summation of bubble contribution (new β), their individual contribution in each single cell is not equal since they have different geometrical shapes (Fig. 1). As a solution, instead of injecting one large bubble, the vapour structure should be replaced by a group of small bubbles which do not occupy more than one cell; this is also consistent with the notion of subgrid scale modelling. The size of new bubbles in each cell are determined based on the old value of α such that the value of $\alpha\beta$ is conserved in that cell. The improved transition approach is shown schematically in Fig. 2. The blue cells include Eulerian cavities and the red ones are occupied by Lagrangian bubbles. In the white cells both α and β are equal to 1. Also, instead of large bubbles, several smaller bubbles are injected, as compared to Fig. 1. This leads to an increase in computational cost, as more bubbles are introduced, but gives a significantly improved representation of the smaller vapour structures. It is important to note that the vapour volume fraction of the small Eulerian cavities are less than one, which means that the cavity is not pure vapour. In other words, during mixture-bubble transition we are dealing with a small cloud of many bubbles (distributed in the surrounding liquid) and not a single bubble full of pure vapour. From the Eulerian mixture it is not possible to obtain the distribution of bubble diameters and positions in this small cloud. However, it is interesting to know that the bubble distribution and sizes do not considerably change the collapse rate of the total cloud from an Eulerian point of view, as inferred from the works of Schmidt et al. [3,32]. In these studies, a group of bubbles with *random distribution* in position and size were simulated both as individual bubbles as well as an equivalent cloud and the results show that both simulations lead to quite similar collapse profile. Therefore, replacing the cavity with more smaller bubbles rather than one single large bubble, not only solve the numerical pressure pulse issue, but also makes the transition more aligned with real physics. The small bubbles can have different distributions in size and position, however, to decrease the computational expenses it is suggested to keep the number of bubbles as low as possible, therefore only one or two bubbles are injected in each cell as in Fig. 2.

Avoiding vapour generation in the bubbly cells is one further improvement needed in the solver. In each computational cell that contains vapour, the cavity structure should be tracked either by the Eulerian transport equation or the Lagrangian bubble tracking algorithm. In other words, there cannot exist an Eulerian cavity in a cell that is occupied by a Lagrangian bubble, and vice versa. To avoid compromising this situation, the mass transfer source term in the volume fraction equation should be omitted in the bubbly cells. Thus, Eq. (6) should be rewritten as

$$\frac{\partial\alpha}{\partial t} + \frac{\partial(\alpha u_i)}{\partial x_i} = \frac{\dot{m}}{\rho_l} * \mathbf{pos}(\beta-1). \tag{12}$$

When there is a bubble in a cell, β is less than 1, therefore the $\mathbf{pos}(\beta-1)$ equals zero and no Eulerian vapour fraction is generated in the cell. Without this modification an Eulerian structure can be generated in bubble host cells, according to Eq. (11), as the flow pressure is usually equal or less than the threshold (vapour) pressure in these cells. Then, the vapour structure in such cells and its contribution to the mixture properties will be considered twice. Besides that, the new Eulerian cavity is small at the time of generation and therefore it will be transformed into a Lagrangian bubble in the next time step and then the new and old bubbles can coalesce and make a larger bubble. And this process would be repeated in each time step by generating new Eulerian structures

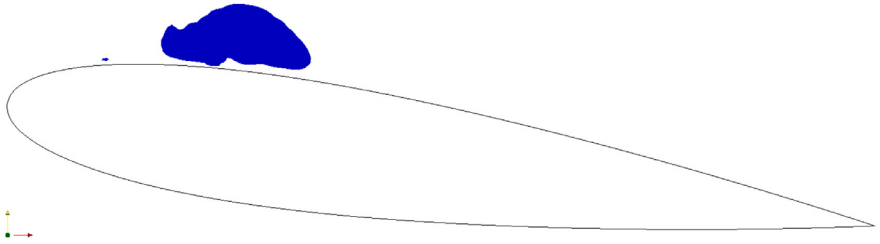

(a)

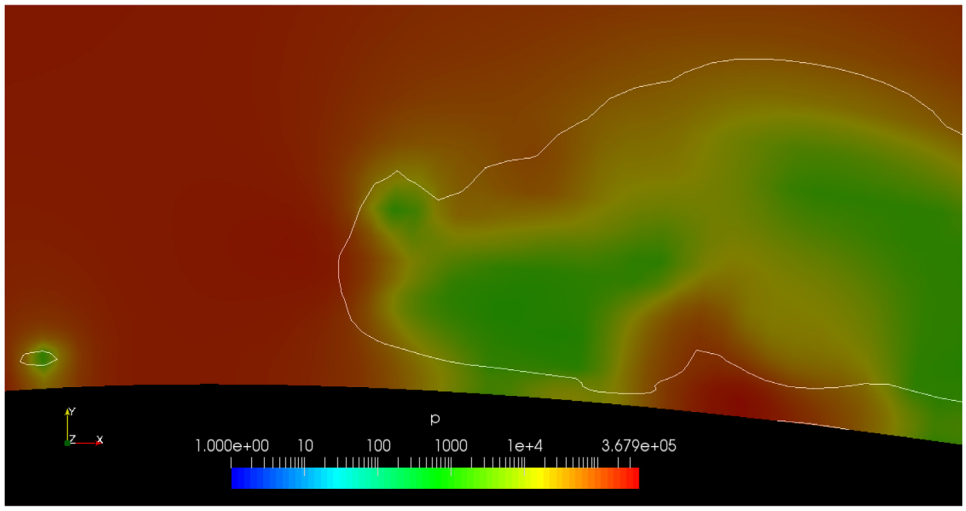

(b)

Fig. 3. (a) Initial cavities with different length scales over a hydrofoil; (b) Initial pressure field, where the line indicates the isocontour of vapour fraction $\alpha = 0.5$. (For interpretation of the references to colour in this figure legend, the reader is referred to the web version of this article.)

which lead to an unstable and unphysical growth of the Lagrangian bubble.

2.5. Solution strategy

The final solution strategy consists of two algorithms. The major algorithm to solve the flow governing equations, and another algorithm for Eulerian–Lagrangian transition. In the developed solver, after initializing of the flow field and defining the solution parameters, in each time step the governing equations are solved in the following order:

Algorithm 1 Solution procedure.

1: **for** `t=start time:end time` **do**
2: Solve Eq. (2) to obtain new velocity field.
3: Find the mass transfer rate, $\dot{m}$, from Eq. (11).
4: Obtain the new pressure field, by solving Eq. (1).
5: Update the mass transfer rate, $\dot{m}$, from Eq. (11).
6: Solve Eq. (12) to find the new liquid volume fraction field.
7: Solve Eqs. (8) and (9) for each bubble to obtain the new positions and diameters.
8: Perform the mixture-bubble transition algorithm (Algorithm 2).
9: Update the mixture properties by solving Eq. (10).
10: **end for**

The second algorithm is the Eulerian mixture -Lagrangian bubble transition algorithm. The original step-by-step transition process is explained by Vallier [12]. However, to meet the currently introduced improvements, the algorithm needs to be revised. Similar to Vallier's approach, in the first step all of the cavity structures in the flow domain are detected. Next, the number of computational cells that resolve each structure are counted. If this number is less than a threshold value (e.g. 5, in this study), it is decided that the relative structure is not resolved by sufficient number of grid cells. Then, for each cavity that is not well resolved, the Algorithm 2 is followed.

Algorithm 2 Transition algorithm.

1: Create a list of cell labels {cell j , j=1:J}, associated with the cavity structure.
2: **for** `j=1:J` **do**
3: Evaluate the cavity volume $V_{vapour,j}$.
4: Find the minimum edge length of the cell, $\Delta_{min,j}$
5: Find the minimum No. of bubble(s) in the cell, N_b, and the largest possible bubble radius, R_b, so that $N_b \frac{4}{3}\pi {R_b}^3 = V_{vapour,j}$,$R_b < \Delta_{min,j}$.
6: **for** `k=1:`N_b **do**
7: Find the bubble position vectors $\mathbf{X}_{b,k}$ in the cell j: The positions vectors are N_b points in the cell volume with uniform distribution.
8: Set the bubble velocity, $\mathbf{U}_b$, equal to the Eulerian mixture velocity in the cell, $\mathbf{U}_j$.
9: Inject the bubble
10: **end for**
11: Remove the Eulerian cavity of the cell by setting $\alpha_j = 1$.
12: **end for**

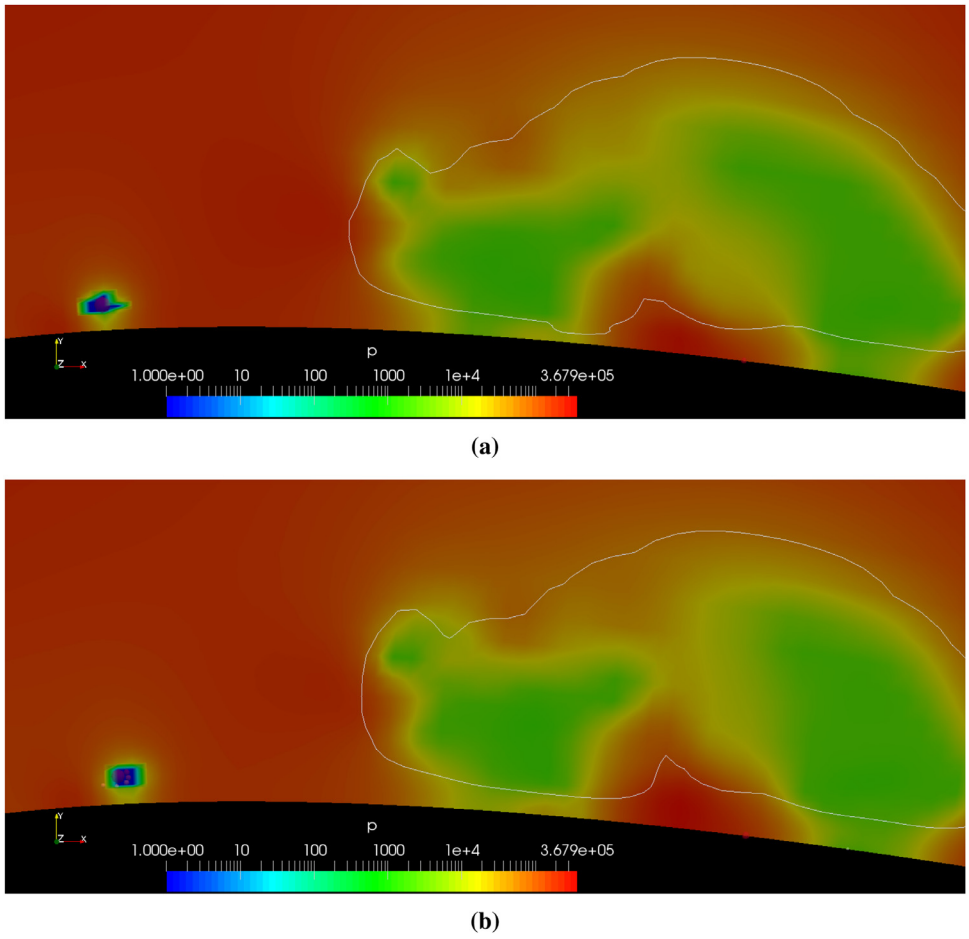

Fig. 4. Pressure field (the line indicates the isocontour of vapour fraction $\alpha = 0.5$) of the original model (a) 1 time step after transition; (b) a few time steps later. Note the blue area (negative pressure) around the large red bubbles. (For interpretation of the references to colour in this figure legend, the reader is referred to the web version of this article.)

Also, if a Lagrangian bubble collides with a large Eulerian cavity, or it becomes large enough to be resolved by sufficient number of cells, it will be transformed to an Eulerian structure by deleting the bubble, while in the host cell β is set to 1 and $\alpha = \beta_{old}$. The transition criteria can be improved in further development of the model, which is the topic of a future study.

3. Result

In this section, the performance of the original and the new realizable multi-scale models are compared for qualitative validation of the proposed improvements. In Fig. 3a, two cavity structures with different length scales are shown over the suction side of a 2D hydrofoil. The large structure should be kept in the Eulerian framework while the smaller one is a candidate to be transformed to the Lagrangian bubble framework. Also, in Fig. 3b, the pressure contour around the cavities before transition is depicted. The contour is plotted in logarithmic scale for easier detection of pressure pulses. Inside the cavities (green area) the pressure is around vapour pressure, which is 2340 Pascal in this problem.

The pressure field after the Eulerian–Lagrangian transition of the original multi-scale model is shown in Fig. 4. Fig. 4a displays the prediction one time step after the transition. As can be seen, the local pressure at the small cavity location decreases to not only smaller than the threshold vapour pressure but also to large negative values. Also, at some time steps later (Fig. 4b), due to the decrease in pressure as well as the mass transfer rate in the α equation (Eq. (6)), new vapour structures are generated which are subsequently transformed to Lagrangian bubbles leading to more pulses in the flow. Such pressure pulses are repeated several times in the domain.

The pressure contour obtained from the realizable model is shown in Fig. 5. Here, the small cavity structure is replaced by more but smaller bubbles in order to keep the $\alpha\beta$ parameter conserved in all cells during the transition. As a result, no pressure pulse or negative pressure is seen in the domain.

To gain a better understanding, in Fig. 6 the minimum pressure of the flow field is shown for 75 time steps after the Eulerian–Lagrangian transition. It is seen that the minimum pressure of the realizable model is approximately constant and is around the threshold vapour pressure, while for the original model, the pressure repeatedly yield large negative values due to several spurious pulses that occur after the transition. Such large negative pressures can influence the noise prediction and erosion estimation of a cavitating flow and if they occur near the hydrofoil, the hydrodynamic force estimation may be affected as well; in the worst case the numerical stability of the solver may be compromised.

In Fig. 7, the local vapour volume as well as the number of Lagrangian bubbles around the transition area are depicted for 75 time steps after the transition. For the realizable model, the Eulerian–Lagrangian transition occurs once and after that no Eulerian vapour cavity is seen in the region and the number of bubbles stays constant. However, for the original model, new vapour cavities are generated in the area several times. As stated above, this vapour generation is due to the mass transfer source term in

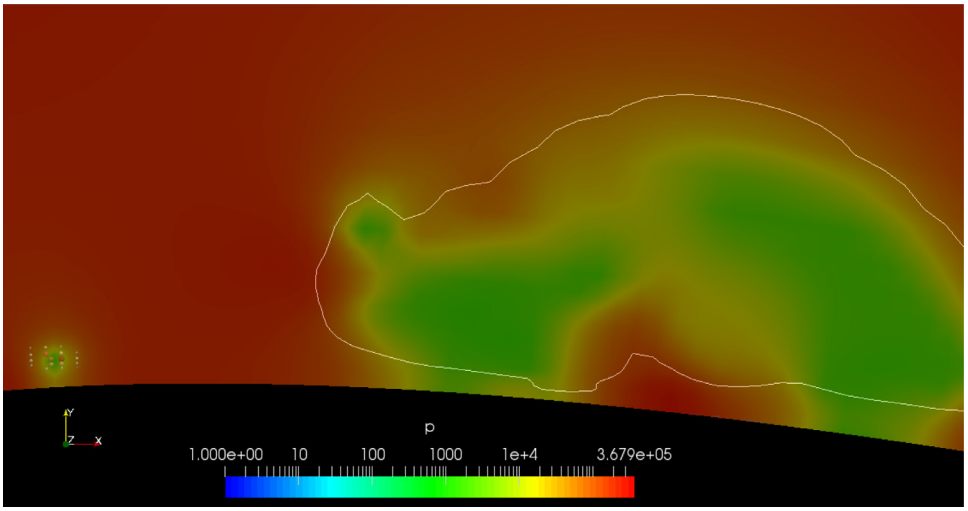

Fig. 5. Pressure contour after the Eulerian–Lagrangian transition of the realizable model; the line indicates the isocontour of vapour fraction $\alpha = 0.5$.

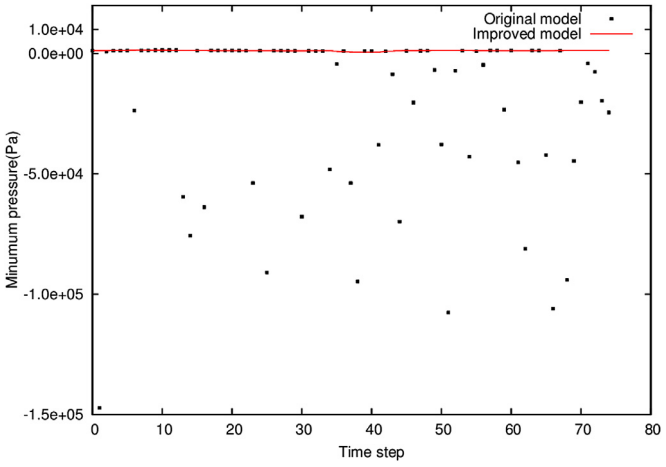

Fig. 6. Minimum pressure after the first transition.

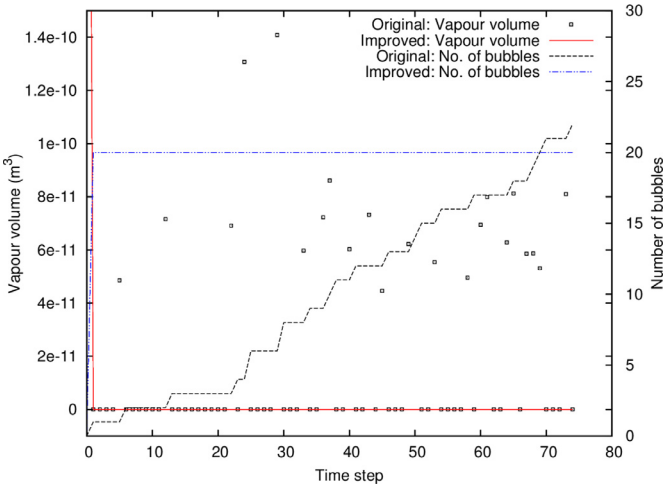

Fig. 7. Vapour volume and number of bubbles after the first transition.

Eq. (6) and the large negative pressure after each transition. As the new cavities are small, they are transformed to Lagrangian bubbles instantaneously which in turn leads to new spurious pulses and yet again vapour generation. Also, the number of Lagrangian bubbles increases in the domain. It should be noted that these bubbles are larger than the corresponding ones in the realizable model. The new bubbles increase the vapour content of the flow and interact with the earlier generated bubbles; both of these effects are unrealistic.

4. Summary

A new multi-scale approach for numerical simulation of cavitating flows has been presented. The coupling of the Eulerian mixture model with the Lagrangian discrete bubble model makes the solver capable of resolving various cavity structures with different length scales, including sub-grid bubbles. An issue in previous attempts at developing such a model has been that the transition of an Eulerian structure to a Lagrangian framework induces spurious pressure pulses and spurious vapour generation. In this paper, we present a remedy to this issue by reformulating the coupling between the bubbles and the Eulerian governing equations to more accurately include the effects of bubbles on the Eulerian flow. This amounts to considering the total vapour on the flow, and not only the Eulerian mixture vapour fraction. Also, several discrete bubbles are inserted to achieve a better representation of the spatial distribution of the Eulerian mixture during the transition. Further, an example of the problem with the previous approach and how the new model overcome this was given through the dynamics of a small shed cavity in the flow over a 2D foil.

In future studies, the hybrid model will be improved further. It includes the improvement of the Lagrangian library in order to estimate the local flow effects on bubble dynamics more accurately, as compared to the previous studies. Also, the model performance will be validated quantitatively with available benchmark studies in literature. The Lagrangian module has the potential to predict the cavitation inception, since the inception sites, nuclei, can be treated as micro bubbles. Besides that, incorporation of the radiated acoustic pressure wave due to bubble collapse and rebound can be used in surface erosion estimation.

Acknowledgements

This work is funded through the H2020 project CaFE, a Marie Skłodowska-Curie Action Innovative Training Network project, grant number 642536.

References

[1] Koop AH. Numerical simulation of unsteady three-dimensional sheet cavitation. Ph.D. thesis, University of Twente; 2008.
[2] Schnerr GH, Sezal IH, Schmidt SJ. Numerical investigation of three-dimensional cloud cavitation with special emphasis on collapse induced shock dynamics. Phys Fluids 2008;20(4):040703.
[3] Schmidt SJ, Mihatsch MS, Thalhamer M, Adams NA. Assessment of erosion sensitive areas via compressible simulation of unsteady cavitating flows. In: Advanced experimental and numerical techniques for cavitation erosion prediction. Springer; 2014. p. 329–44.
[4] Bensow RE, Bark G. Implicit les predictions of the cavitating flow on a propeller. J Fluids Eng 2010;132(4):041302.
[5] Asnaghi A, Feymark A, Bensow R. Improvement of cavitation mass transfer modeling based on local flow properties. Int J Multiphase Flow 2017;93:142–57.
[6] Singhal AK, Athavale MM, Li H, Jiang Y. Mathematical basis and validation of the full cavitation model. Trans Am Soc MechEng J Fluids Eng 2002;124(3):617–24.
[7] Yakubov S, Maquil T, Rung T. Experience using pressure-based cfd methods for euler–euler simulations of cavitating flows. Comput Fluids 2015;111:91–104.
[8] Lauer E, Hu X, Hickel S, Adams NA. Numerical modelling and investigation of symmetric and asymmetric cavitation bubble dynamics. Comput Fluids 2012;69:1–19.
[9] Abdel-Maksoud M, Hänel D, Lantermann U. Modeling and computation of cavitation in vortical flow. Int J Heat Fluid Flow 2010;31(6):1065–74.
[10] Giannadakis E, Gavaises M, Arcoumanis C. Modelling of cavitation in diesel injector nozzles. J Fluid Mech 2008;616:153–93.
[11] Hsiao C-T, Ma J, Chahine GL. Simulation of sheet and tip vortex cavitation on a rotating propeller using a multiscale two-phase flow model. Fourth int. symp. mar. propulsors, Austine, Texas, USA; 2015.
[12] Vallier A. Simulations of cavitation-from the large vapour structures to the small bubble dynamics. Ph.D. thesis, Lund University; ISBN 978-91-473-517-8, 2013.
[13] Tomar G, Fuster D, Zaleski S, Popinet S. Multiscale simulations of primary atomization. Comput Fluids 2010;39(10):1864–74.
[14] Tomiyama A, Shimada N. Two-fluid model with interface sharpening. JComputFluid Dyn 2001;9(4):418–26.
[15] Černe G, Petelin S, Tiselj I. Coupling of the interface tracking and the two-fluid models for the simulation of incompressible two-phase flow. J Comput Phys 2001;171(2):776–804.
[16] Štrubelj L, Tiselj I. Two-fluid model with interface sharpening. Int J Numer Methods Eng 2011;85(5):575–90.
[17] Jiang X, Siamas G, Jagus K, Karayiannis T. Physical modelling and advanced simulations of gas–liquid two-phase jet flows in atomization and sprays. Prog Energy Combust Sci 2010;36(2):131–67.
[18] Kim D, Herrmann M, Moin P. The breakup of a round liquid jet by a coaxial flow of gas using the refined level set grid method. APS division of fluid dynamics meeting abstracts; 2006.
[19] Herrmann M. A parallel Eulerian interface tracking/lagrangian point particle multi-scale coupling procedure. J Comput Phys 2010;229(3):745–59.
[20] Ling Y, Zaleski S, Scardovelli R. Multiscale simulation of atomization with small droplets represented by a lagrangian point-particle model. Int J Multiphase Flow 2015;76:122–43.
[21] Grosshans H, Szász R-Z, Fuchs L. Development of an efficient statistical volumes of fluid–lagrangian particle tracking coupling method. Int J Numer Methods Fluids 2014;74(12):898–918.
[22] Ström H, Sasic S, Holm-Christensen O, Shah LJ. Atomizing industrial gas-liquid flows–development of an efficient hybrid vof-lpt numerical framework. Int J Heat Fluid Flow 2016;62:104–13.
[23] Hsiao C-T, Ma J, Chahine GL. Multiscale tow-phase flow modeling of sheet and cloud cavitation. Int J Multiphase Flow 2017;90:102–17.
[24] Ma J, Hsiao C-T, Chahine GL. A physics based multiscale modeling of cavitating flows. Comput Fluids 2017;145:68–84.
[25] OpenFoam. The Open Source CFD Toolbox openfoam foundation. http://www.openfoam.com; Accessed: 2018-01-15, 2018.
[26] Schnerr GH, Sauer J. Physical and numerical modeling of unsteady cavitation dynamics. Fourth international conference on multiphase flow, New Orleans, USA, 1; 2001.
[27] Liu AB, Mather D, Reitz RD. Modeling the effects of drop drag and breakup on fuel sprays. Tech. Rep. Wisconsin Univ-Madison Engine Research Center; 1993.
[28] Mei R. An approximate expression for the shear lift force on a spherical particle at finite reynolds number. Int J Multiphase Flow 1992;18(1):145–7.
[29] Franc J-P, Michel J-M. Fundamentals of Cavitation, 76. Springer Science & Business Media; 2006.
[30] Plesset MS, Prosperetti A. Bubble dynamics and cavitation. Annu Rev Fluid Mech 1977;9(1):145–85.
[31] Shampine LF, Reichelt MW. The matlab ode suite. SIAM JSciComput 1997;18(1):1–22.
[32] Schmidt S, Mihatsch M, Thalhamer M, Adams N. Assessment of the prediction capability of a thermodynamic cavitation model for the collapse characteristics of a vapor-bubble cloud. WIMRC 3rd international cavitation forum. University of Warwick UK; 2011.